

## Adaptive venom evolution and toxicity in octopods is driven by extensive novel gene formation, expansion and loss --Manuscript Draft--

<b>Manuscript Number:</b>	GIGA-D-20-00135R2	
<b>Full Title:</b>	Adaptive venom evolution and toxicity in octopods is driven by extensive novel gene formation, expansion and loss	
<b>Article Type:</b>	Research	
<b>Funding Information:</b>	Australian Biological Resources Study (ref:RF211-41)	Assoc Prof Jan M. Strugnell
	Austrian Science Fund (FWF) grant (P30686-B29)	Prof Oleg Simakov
<b>Abstract:</b>	<p><b>Background</b></p> <p>Cephalopods represent a rich system for investigating the genetic basis underlying organismal novelties. This diverse group of specialised predators has evolved many adaptations including proteinaceous venom. Of particular interest is the blue-ringed-octopus genus ( <i>Hapalochlaena</i> ), which are the only octopods known to store large quantities of the potent neurotoxin, tetrodotoxin, within their tissues and venom gland.</p> <p><b>Findings</b></p> <p>To reveal genomic correlates of organismal novelties, we conducted a comparative study of three octopod genomes, including the Southern blue-ringed octopus ( <i>Hapalochlaena maculosa</i> ). We present the genome of this species and reveal highly dynamic evolutionary patterns at both non-coding and coding organizational levels. Gene family expansions previously reported in <i>Octopus bimaculoides</i> (e.g., zinc finger and cadherins, both associated with neural functions), as well as formation of novel gene families, dominate the genomic landscape in all octopods. Examination of tissue-specific genes in the posterior salivary gland (PSG) revealed that expression was dominated by serine proteases in non- tetrodotoxin bearing octopods, while this family was a minor component in <i>H. maculosa</i> . Moreover, voltage-gated sodium channels in <i>H. maculosa</i> contain a resistance mutation found in pufferfish and garter snakes, which is exclusive to the genus. Analysis of the PSG microbiome revealed a diverse array of bacterial species, including genera that can produce tetrodotoxin, suggestive of a possible production source.</p> <p><b>Conclusions</b></p> <p>We present the first tetrodotoxin-bearing octopod genome <i>H. maculosa</i>, which displays lineage-specific adaptations to tetrodotoxin acquisition. This genome, along with other recently published cephalopod genomes, represents a valuable resource from which future work could advance our understanding of the evolution of genomic novelty in this family.</p>	
<b>Corresponding Author:</b>	Brooke Lauren Whitelaw, Bachelor with Honours and current PhD candidate James Cook University College of Science and Engineering Townsville, QLD AUSTRALIA	
<b>Corresponding Author Secondary Information:</b>		
<b>Corresponding Author's Institution:</b>	James Cook University College of Science and Engineering	
<b>Corresponding Author's Secondary Institution:</b>		
<b>First Author:</b>	Brooke Lauren Whitelaw	
<b>First Author Secondary Information:</b>		
<b>Order of Authors:</b>	Brooke Lauren Whitelaw	

	Ira R. Cooke
	Julian Finn
	Rute R. da Fonseca
	Elena A. Ritschard
	M. T P. Gilbert
	Oleg Simakov
	Jan M. Strugnell
<b>Order of Authors Secondary Information:</b>	
<b>Response to Reviewers:</b>	<p>We would like to thank the reviewers for their helpful comments, which have been addressed below and the editor for considering our manuscript for publication.</p> <p>Reviewer reports:</p> <p>Reviewer #1: The authors have made the changes that I requested. I confess that I did not carefully read through the revision to verify that all of the minor grammatical edits I proposed were made, but I "spot checked" several and they look pretty good.</p> <p>Reviewer #2: The authors have adequately revised their manuscript in response to my review and addressed the comments in my review with their letter. I have just two minor suggestions after reading the revised manuscript.</p> <p>1) The authors should choose one convention for spelling the word specialized either specialised (British) or specialized (American).</p> <p>We have chosen to use the British spelling and corrected the one American spelling at pg. 1, line 24.</p> <p>2) In lines 372-374, the authors comment on the interactions between aspartic acid and TTX, "While it has yet to be assessed for TTX resistance, the replacement of Asp in <i>B. candida</i> with a neutral amino acid has been predicted to disrupt TTX binding by preventing formation of a hydrogen bond." A better reference for this statement is Shen et al. (2018). In addition, the cryo-EM structure data from this paper suggest that either a hydrogen bond or a salt bridge could form between TTX and that aspartic acid at this position of the protein.</p> <p>We agree that this sentence required clarification, specifically that both hydrogen and salt bridges could be disrupted. This information has been added to the modified sentence as well as the suggested reference.</p> <p>Original sentence:  "While it has yet to be assessed for TTX resistance, the replacement of Asp in <i>B. candida</i> with a neutral amino acid has been predicted to disrupt TTX binding by preventing formation of a hydrogen bond<sup>90</sup>"</p> <p>Revised sentence: (pg. 17, lines : 396-398)  "While it has yet to be assessed for TTX resistance, the replacement of Asp in <i>B. candida</i> with a neutral amino acid has been predicted to disrupt TTX binding by preventing formation of a salt bridge or hydrogen bond<sup>89,91</sup>"</p>
<b>Additional Information:</b>	
<b>Question</b>	<b>Response</b>
Are you submitting this manuscript to a special series or article collection?	No
<b>Experimental design and statistics</b>	Yes

<p>Full details of the experimental design and statistical methods used should be given in the Methods section, as detailed in our <a href="#">Minimum Standards Reporting Checklist</a>. Information essential to interpreting the data presented should be made available in the figure legends.</p> <p>Have you included all the information requested in your manuscript?</p>	
<p><b>Resources</b></p> <p>A description of all resources used, including antibodies, cell lines, animals and software tools, with enough information to allow them to be uniquely identified, should be included in the Methods section. Authors are strongly encouraged to cite <a href="#">Research Resource Identifiers</a> (RRIDs) for antibodies, model organisms and tools, where possible.</p> <p>Have you included the information requested as detailed in our <a href="#">Minimum Standards Reporting Checklist</a>?</p>	<p>Yes</p>
<p><b>Availability of data and materials</b></p> <p>All datasets and code on which the conclusions of the paper rely must be either included in your submission or deposited in <a href="#">publicly available repositories</a> (where available and ethically appropriate), referencing such data using a unique identifier in the references and in the “Availability of Data and Materials” section of your manuscript.</p> <p>Have you have met the above requirement as detailed in our <a href="#">Minimum Standards Reporting Checklist</a>?</p>	<p>Yes</p>

1 **Adaptive venom evolution and toxicity in octopods is driven by**  
2 **extensive novel gene formation, expansion and loss**

3 Brooke L. Whitelaw<sup>1,2,\*</sup>, Ira R. Cooke<sup>3,4</sup>, Julian Finn<sup>2</sup>, Rute R. da Fonseca<sup>5</sup>, Elena A.

4 Ritschard<sup>6,7</sup>, M. T P. Gilbert<sup>8</sup> Oleg Simakov<sup>6</sup>, Jan M. Strugnell<sup>1,9</sup>

5

6 <sup>1</sup>Centre for Sustainable Tropical Fisheries and Aquaculture, James Cook University,

7 Townsville, Queensland, 4811, Australia

8 <sup>2</sup>Sciences, Museum Victoria, Carlton, Victoria 3053, Australia

9 <sup>3</sup>College of Public Health, Medical and Vet Sciences, James Cook University,

10 Townsville, Queensland, 4811, Australia

11 <sup>4</sup>La Trobe Institute of Molecular Science, La Trobe University, Melbourne, Victoria

12 3086, Australia

13 <sup>5</sup>Center for Macroecology, Evolution and Climate (CMEC), GLOBE Institute, University

14 of Copenhagen, Universitetsparken 15, 2100 Copenhagen, Denmark;

15 <sup>6</sup>Department of Neurosciences and Developmental Biology, University of Vienna,

16 Austria



17 <sup>7</sup>Department of Biology and Evolution of Marine Organisms, Stazione Zoologica Anton

18 Dohrn, Italy

19 <sup>8</sup>Center for Evolutionary Hologenomics, GLOBE Institute, University of Copenhagen,

20 Øster Voldgade 5-7, 1350 Copenhagen, Denmark;

21 <sup>9</sup>Department of Ecology, Environment and Evolution, La Trobe University, Melbourne,

22 Victoria, 3086 Australia

23

24 \*Brooke Whitelaw,Email: 1blwhitelaw8@gmail.com,Phone number: 0424642621

25

26 ORCIDs:

27 Brooke L. Whitelaw, 0000-0002-5555-4612;

28 Ira R. Cooke, 0000-0001-6520-1397;

29 Julian Finn, 0000-0003-1820-512X;

30 Rute R. da Fonseca, 0000-0002-2805-4698;

31 Elena A. Ritschard, 0000-0002-4956-9703;

32 M. T P. Gilbert, 0000-0002-5805-7195;

33 Oleg Simakov, 0000-0002-3585-4511;

34 Jan M. Strugnell, 0000-0003-2994-637X.

35

36 ***Abstract***

37 ***Background***

38 Cephalopods represent a rich system for investigating the genetic basis underlying  
39 organismal novelties. This diverse group of specialised predators has evolved many  
40 adaptations including proteinaceous venom. Of particular interest is the blue-ringed-  
41 octopus genus (*Hapalochlaena*), which are the only octopods known to store large  
42 quantities of the potent neurotoxin, tetrodotoxin, within their tissues and venom gland.

43 ***Findings***

44 To reveal genomic correlates of organismal novelties, we conducted a comparative  
45 study of three octopod genomes, including the Southern blue-ringed octopus  
46 (*Hapalochlaena maculosa*). We present the genome of this species and reveal highly  
47 dynamic evolutionary patterns at both non-coding and coding organizational levels.  
48 Gene family expansions previously reported in *Octopus bimaculoides* (e.g., zinc finger  
49 and cadherins, both associated with neural functions), as well as formation of novel

50 gene families, dominate the genomic landscape in all octopods. Examination of tissue-  
51 specific genes in the posterior salivary gland (PSG) revealed that expression was  
52 dominated by serine proteases in non- tetrodotoxin bearing octopods, while this family  
53 was a minor component in *H. maculosa*. Moreover, voltage-gated sodium channels in *H.*  
54 *maculosa* contain a resistance mutation found in pufferfish and garter snakes, which is  
55 exclusive to the genus. Analysis of the PSG microbiome revealed a diverse array of  
56 bacterial species, including genera that can produce tetrodotoxin, suggestive of a  
57 possible production source.

## 58 ***Conclusions***

59 We present the first tetrodotoxin-bearing octopod genome *H. maculosa*, which displays  
60 lineage-specific adaptations to tetrodotoxin acquisition. This genome, along with other  
61 recently published cephalopod genomes, represents a valuable resource from which  
62 future work could advance our understanding of the evolution of genomic novelty in  
63 this family.

64

## 65 ***Background***

66 Reconstructing the evolution of novelties at the genomic level is becoming an  
67 increasingly viable approach to understand their origin. The recent publication of  
68 octopod genomes provides an opportunity to investigate the link between genomic and  
69 organismal evolution in this unique lineage for which genomic resources have been  
70 lacking[1]. From their emergence 275 mya[2], octopods have diversified into > 300  
71 species, inhabiting tropical to polar regions, from the deep sea to shallow intertidal  
72 zones[3]. As a highly diverse group, octopods show remarkable variation in body form  
73 and function. They are specialised soft-bodied predators that are well adapted to their  
74 environment with prehensile limbs lined with chemosensory suckers[4], the ability to  
75 manipulate skin texture and colour using specialised chromatophores[5], the largest  
76 invertebrate nervous systems (excluding those of other cephalopods)[6], and a  
77 relatively large circumesophageal brain allowing for complex problem solving and  
78 retention of information[7]. Furthermore, the cephalopods have independently evolved  
79 proteinaceous venom, which is produced and stored within a specialised gland in  
80 known as the posterior salivary gland (PSG). All octopods are believed to possess a  
81 form of proteinaceous venom used to subdue prey[8–10]. Serine proteases are a  
82 common component of cephalopod venoms and have been observed in the PSG of

83 squids, cuttlefish and octopods[10–13]. Convergent recruitment of serine proteases has  
84 been observed between many vertebrate (Squamata[14–16] and Monotremata[17])  
85 and invertebrate (Hymenoptera[18], Arachnida[19], Gastropoda[20], Remipedia[21]  
86 and Cnidarian[22]) venomous lineages.

87         In addition to these proteinaceous venoms, the blue-ringed octopus (genus  
88 *Hapalochlaena*) is the only group that also contains the potent non-proteinaceous  
89 neurotoxin, tetrodotoxin (TTX)[12,23]. The mechanism of TTX resistance, which allows  
90 for safe sequestration of TTX, has been attributed to several substitutions in the p-loop  
91 regions of voltage-gated sodium channels( $\text{Na}_v$ ) in *H. lunulata*[24]. However, these  
92 channels have yet to be examined in *H. maculosa* and *H. fasciata*. TTX resistance has  
93 also been studied in a range of other genera including, pufferfish[25], newts[26,27]  
94 arachnids[28], snakes[29] and gastropods[30].

95         The blue-ringed octopus is easily identified by iridescent blue rings, which  
96 advertise its toxicity in an aposematic display[31–33]. Sequestration of the TTX within  
97 bodily tissues is unique to this genus among cephalopods[32,34]. While other  
98 unrelated TTX-bearing species primarily use TTX for defense, *Hapalochlaena* is the only  
99 known taxa to utilise TTX in venom[23,35]. The impact of TTX inclusion on venom

100 composition and function has been previously investigated in the southern blue-ringed  
101 octopus (*H. maculosa*)[9]. Relative to the non-TTX bearing species *Octopus kaurna*, *H.*  
102 *maculosa* exhibited greater expression of putative dispersal factors such as  
103 hyaluronidase, which serve to aid in the dispersal of toxic venom components[9].  
104 Conversely, tachykinins- neurotoxins known from other octopods[36,37] were absent  
105 from the *H. maculosa* PSG[9]. Further investigation into the broader impact of TTX on  
106 the evolutionary trajectory of the species has yet to be addressed due to the absence of  
107 a genome.

108         This study presents the genome of the southern blue-ringed octopus (*H.*  
109 *maculosa*, NCBI:txid61716; marinespecies.org:taxname:342334), the first from the  
110 genus *Hapalochlaena*. By using a comparative genomic approach we are able to  
111 examine the emergence of octopod novelties, at a molecular level between *H. maculosa*  
112 and the two non-TTX bearing octopods: the California two-spot octopus (*O.*  
113 *bimaculoides*) and the long-armed octopus (*Callistoctopus minor*). We also address unique  
114 features of venom evolution in octopods while also addressing the species-specific  
115 evolution of tetrodotoxin acquisition and resistance in *H. maculosa*.

116

117 *Keywords:* cephalopod genome, comparative genomics, gene family expansions,  
118 transposable elements, venom evolution

119

120

## 121 ***Data Description***

### 122 ***Genome assembly and annotation***

123         The southern blue-ringed octopus genome was sequenced using Illumina paired  
124 end and Dovetail sequencing from a single female collected at Beaumaris Sea Scout  
125 Boat Shed, Beaumaris, Port Phillip Bay, Victoria, Australia. The assembly was  
126 composed of 48,285 scaffolds with an N50 of 0.93 Mb and total size of 4.08 GB. A total  
127 of 29,328 inferred protein coding genes were predicted using a PASA[38] and an  
128 Augustus[39] pipeline and supplemented with zinc finger and cadherin genes obtained  
129 from aligning *H. maculosa* transcripts to *O. bimaculoides* gene models(Supplementary  
130 notes 1.1-1.4). Completeness of the genome was estimated using BUSCO[40], which  
131 identified 87.7% complete and 7.5% fragmented genes against the metazoan database  
132 of 978 groups (Supplementary notes 3.2).

133 *H. maculosa* has a highly heterozygous genome (0.95%), similar to *O. vulgaris*  
134 (1.1%)[41] but far higher than *O. bimaculoides* (0.08%)[42]. While the low  
135 heterozygosity of *O. bimaculoides* is surprising, other molluscs also have highly  
136 heterozygous genomes in accordance with *H. maculosa*, including the gastropods (1-  
137 3.66%)[43,44] and bivalves (0.51-3%)[45–51](Supplementary table 5).

138

### 139 ***PSMC (Pairwise Sequentially Markovian Coalescent) and mutation rate***

140 The mutation rate for *H. maculosa* was estimated to be  $2.4 \times 10^{-9}$  per site per  
141 generation based on analysis of synonymous differences with *O. bimaculoides*  
142 (Supplementary note 1.5). The mutation rate is comparable to the average mammalian  
143 mutation rate of  $2.2 \times 10^{-9}$  per site per generation, and *Drosophila*,  $2.8 \times 10^{-9}$ [52,53].  
144 Due to the unavailability of a suitable closely related and comprehensive genome until  
145 the publication of *O. bimaculoides* in 2015[42], this is the first genome-wide mutation  
146 rate estimated for any cephalopod genome.

147 The historic effective population size ( $N_e$ ) of *H. maculosa* was estimated using  
148 the pairwise sequentially Markovian coalescent (PSMC) model (Supplementary Fig 2).  
149 Population size was found to initially increase during the early Pleistocene, followed by



150 a steady decline which slows slightly around 100kya. Note that PSMC estimates are not  
151 reliable at very recent times due to a scarcity of genomic blocks that share a recent  
152 common ancestor in this highly heterozygous genome. A decline in population size  
153 started during the mid-Pleistocene approximately 1mya, a time of unstable  
154 environmental conditions with fluctuations in both temperature and glaciation  
155 events[54–56]. Corals in the genus *Acropora* show a similar pattern of expansion and  
156 contraction attributed to niche availability post mass extinction of shallow-water  
157 marine organisms 2-3 mya, followed by the unstable mid-Pleistocene climate[57,58]. A  
158 similar pattern of expansion and decline in effective population size has also been  
159 observed in the Antarctic ice fish among other marine organisms distributed in the  
160 Southern Hemisphere[59].

161

## 162 ***Phylogenomics***

163 A total of 2,108 (single copy/ 1-to-1) orthologous clusters were identified  
164 between the molluscan genomes and transcriptomes of 11 species and used to construct  
165 a time-calibrated maximum likelihood tree(Fig 1a). The phylogenetic reconstruction  
166 estimated the divergence time between *H. maculosa* and its nearest relative, *O.*

167 *bimaculoides*, to be ~59 mya. *C. minor* diverged from this clade much earlier ~183  
168 mya. Previous phylogenies using a combination of a small number of mitochondrial  
169 and nuclear genes[60–62] and orthologs derived from transcriptomes[63] support this  
170 topology. Likewise, estimates by Tanner et al.<sup>2</sup>, using a concatenated alignment of 197  
171 genes with a Bayesian approach, placed divergence of *H. maculosa* from *Abdopus*  
172 *aculeatus* at ~59 mya[2].

173 Inference of “shared” phenotypic traits can be difficult to resolve with the  
174 current literature. For example, false eye spots/ocelli observed in both *O. bimaculoides*  
175 and *H. maculosa* are structurally very different. Each ocellus in *H. maculosa* is composed  
176 of a continuous single blue ring[33], while *O. bimaculoides* has a blue ring composed of  
177 multiple small rings. Morphological variations of ocelli structure and colour, in  
178 conjunction with the taxonomically sporadic occurrence of this trait across species  
179 within *Octopus* and *Amphioctopus*, limits our interpretation as to the evolutionary  
180 history of this trait in octopods[3] . Large gaps remain in the literature between  
181 phenotypic traits in cephalopods and their genomic source[1]. This study aims to  
182 provide a genomic framework to enable resolution of these features by profiling

183 changes in several genomic characters: (i) gene duplications, (ii) novel gene formation,  
184 and (iii) non-coding element evolution.

185

186 **Fig 1. Comparisons of molluscan genomes and gene families** a) Time-calibrated maximum likelihood  
187 phylogeny of seven molluscan genomes (*Aplysia californica*, *Lottia gigantea*, *Crassostrea gigas*, *Euprymna*  
188 *scolopes*, *Octopus bimaculoides*, *Callistoctopus minor* and *Hapalochlaena maculosa*) and four transcriptomes  
189 (*Octopus kaurna*, *Octopus vulgaris*, *Sepia officinalis* and *Idiosepius notoides*) using 2,108 single copy  
190 orthologous sequence clusters. Node labels show divergence times in millions of years (mya), blue  
191 (divergence to octopods) and orange bars (decapods) represent standard error within a 95% confidence  
192 interval. Octopodiformes lineages are highlighted in blue and decapod orange. Scale bar represents  
193 millions of year (mya). b) Expansions of octopod gene families relative to molluscan genomes *Aplysia*  
194 *californica* (A. cali), *Biomphalaria glabrata* (B. glab), *Crassostrea gigas* (C. gig), *Lottia gigantea* (L. gig),  
195 *Euprymna scolopes* (E. scol) c) Lineage-specific gene expansions in the octopod genomes *Callistoctopus*  
196 *minor* (C. min), *Octopus bimaculoides* (O. bim) and *Hapalochlaena maculosa* (H. mac). Domains  
197 abbreviated: Chondroitin N-acetylgalactosaminyltransferase (CHGN), C2H2(Cys2-His2) zinc finger and  
198 Cornifin SPRR(small proline-rich proteins).

199

200 ***Organismal impact of novel genes and gene family expansions***

201 Gene family expansions between octopods (*O. bimaculoides*, *C. minor* and *H.*  
202 *maculosa*) and three other molluscan genomes (*Aplysia californica*, *Lottia gigantea* and  
203 *Crassostrea gigas*) were examined using Pfam annotations. A total of 5565 Pfam  
204 domains were identified among six molluscan genomes. *H. maculosa* and *C. minor*  
205 exhibit expansions in the cadherin gene family, characteristic of other octopod  
206 genomes, including *O. bimaculoides* (Fig1b)[42,64]. *C. minor*, in particular, shows the  
207 greatest expansion of this family within octopods. Expansions of protocadherins, a  
208 subset of the cadherin family, have also occurred independently in squid[42], with the  
209 octopod expansions occurring post divergence ~135 mya[42]. The shared ancestry of  
210 octopod cadherins was also documented by Styfhals et al[64] using phylogenetic  
211 inference between *O. bimaculoides* and *O. vulgaris*. Cadherins, specifically  
212 protocadherins, play crucial roles in synapse formation, elimination and axon targeting  
213 within mammals and are essential mediators of short-range neuronal connections[65–  
214 68]. It should be noted that octopods lack a myelin sheath, as a result short-range  
215 connections are integral to maintaining signal fidelity over distance[6]. The  
216 independent expansions of protocadherins within chordate and cephalopod lineages are  
217 believed to be associated with increased neuronal complexity[42,64]. Elevated

218 expression of protocadherins within neural tissues have been observed in *O. vulgaris*  
219 and *O. bimaculoides* by both Styfhals et al[64] and Albertin et al[42] respectively. In  
220 particular Styfhals et al[64] noted differential expression across neural tissues  
221 including supra-esophageal mass, sub-esophageal mass, optic lobe and the stellate  
222 ganglion[64]. However, functional implications of observed expression patterns remain  
223 speculative without further study.

224 *H. maculosa* also shows expansions in the C2H2-type zinc finger family. Zinc  
225 fingers form an ancient family of transcription factors, which among other roles serve  
226 to regulate transposon splicing as well as embryonic and neural development[69,70].  
227 Expansion of this type of zinc finger in *O. bimaculoides* has been associated with neural  
228 tissues. It should be noted that due to the inherent difficulty in fully annotating the  
229 zinc finger family, alternative methods were used to examine the number of exons in *C.*  
230 *minor* with high similarity to annotated zinc finger genes in *O. bimaculoides*  
231 (Supplementary notes 5.1). A total of 609 exons (not captured by published gene  
232 models) from *C. minor* were found with high similarity to accepted zinc finger genes in  
233 *O. bimaculoides*, suggesting this family is larger than that which the genome annotation  
234 infers.

235 Examination of genes specifically expressed within neural tissues found that  
236 cadherins were among the most highly expressed gene families of all octopod species.  
237 Particularly in *C. minor*, relative to the other octopods, such a trend reflects the gene  
238 family expansions found in this species (Fig2c). Zinc fingers were less pronounced,  
239 representing 1.1% of overall expression in *C. minor* compared to cadherins at 11.3%.  
240 Overall, neural tissues express a large diversity of Pfams with each species, exhibiting a  
241 similar profile and proportion of orthologous to lineage-specific genes.

242

### 243 ***Novel patterns of gene expression***

244 High-level examination of gene dynamics (expression, loss of expression and  
245 absence of expression) between octopods across different levels of orthology provides  
246 insight into large-scale expression patterns and highlights lineage-specific loss of  
247 expression.

248 The greatest proportion of genes in each species examined were not specific to  
249 octopods or an octopus lineage (ancient genes) (Fig 2a). Expression of these genes were  
250 enriched in neural tissues across all species, indicating the core conservation of neural  
251 development and function. However, we also find that genes specific to each octopod

252 species also show this expression pattern. The overall elevated expression of genes  
253 within neural tissues could be reflective of the extensive neural network present in  
254 cephalopods, which comprises around 520 million nerve cells[71], rivalling  
255 vertebrates/mammals in size[6]. Expression of many novel genes in the nervous system  
256 may also indicate contribution of those genes to lineage-specific neural network  
257 evolution. In contrast, genes that date back to the shared octopod ancestor show  
258 highest expression in male reproductive tissues in all species.

259 Loss of expression between octopod genomes is exhibited most clearly in *H. maculosa*  
260 with 11% (1993 genes) of all ancient genes having no expression, compared to 1% in  
261 both *O. bimaculoides* and *C. minor*. Absence of gene expression for genes whose  
262 orthologs have retained expression in one or more other species suggests a unique  
263 evolutionary trajectory from other octopods. It should be noted that differences in  
264 tissue sampling may in part influence these values and due to the limited sampling of  
265 species, loss of expression cannot be inferred at a species level and may have occurred  
266 at any point in the lineage. In order to fully understand the implications of the gene  
267 family contractions and loss of expression in *H. maculosa*, relative to other octopods,  
268 further investigation is required.

269

270 **Fig2. Dynamics of gene expression in octopod genomes.** Proportion of gene expression across levels  
271 of specificity from not specific to octopods or an octopus species (left) to octopod-specific (middle) and  
272 lineage-specific (right). Donut plots show gene expression as some expression in any tissue (purple), no  
273 expression (blue) or expression that has been lost (dark blue). Loss of expression requires an ortholog of  
274 the gene to be expressed in one or more species and not expressed in the other species. Heatmaps at each  
275 specificity level show average expression of genes within their respective tissues, low expression (cream)  
276 to high expression (dark red).

277

278 **Fig3. Dynamics of gene expression in neural and venom producing tissues of octopods.** a) Tissue  
279 specific expression of genes within the brain of *H. maculosa*, *O. bimaculoides* and *C. minor* (red). Venn  
280 diagram shows numbers of shared and exclusive genes between species (Left). Bar chart of the top 5  
281 Pfams and their contribution to overall expression in the brain (right). b) Tissue specific expression of  
282 genes within the posterior salivary gland (PSG) of *H. maculosa*, *O. bimaculoides* and *C. minor* (Blue). Venn  
283 diagram shows numbers of shared and exclusive genes between species (left). Bar chart of the top 5  
284 Pfams and their contribution to overall expression in the PSG (right).

285

286 ***Evolution of the octopod non-coding genome***



287            Similar to other cephalopod genomes, the *H. maculosa* genome has a high repeat  
288 content of 37.09% (bases masked). *O bimaculoides* and *C. minor* are also highly  
289 repetitive with 46.39% and 44% of their genomes composed of transposable elements  
290 (TE) respectively. Of the repetitive elements, LINEs dominate the decapodiform  
291 *Euprymna scolopes* genome accounting for its larger genome size[72], while SINEs are  
292 expanded in all four octopod genomes. SINEs have been previously documented in *O.*  
293 *bimaculoides* (7.86%)[42], comparable with *H. maculosa* (7.53%), while fewer SINEs  
294 were previously reported for *C. minor* (4.7%)[73]. SINE elements also dominate the *O.*  
295 *vulgaris* genome with an expansion occurring post divergence from *O. bimaculoides*[41].  
296 Rolling circle (RC) elements are a prominent minor component in octopods,  
297 particularly in *H. maculosa*. RC transposons have been isolated from plant (*Zea mays*)  
298 and mammalian genomes. They depend greatly on proteins used in host DNA  
299 replication and are the only known class of eukaryotic mobile element (transposon) to  
300 have this dependence[74]. TE elements in cephalopod lineages show differing  
301 expansions between most of the genomes currently available, suggesting they are  
302 highly active and play a strong role in cephalopod evolution.

303           Enrichment of transposable elements associated with genes (flanking regions  
304 10kb up- and downstream) was not observed compared to the whole genome for any  
305 species examined. More notable were differences between species, in particular *C.*  
306 *minor* shows a greater proportion of LINE to SINE elements relative to both *O.*  
307 *bimaculoides* and *H. maculosa*.

308           Together, this highlights a very dynamic evolutionary composition of repeats in  
309 cephalopods, that requires further study to test for any potential association with  
310 changes in gene expression or genome evolution.

311

### 312 ***Dynamics of gene expression in the posterior salivary gland (PSG)***

313           The posterior salivary gland is the primary venom-producing gland in octopods.  
314 Venom composition in the majority of octopods is primarily composed of proteinaceous  
315 toxins. *Hapalochlaena* is an exception containing an additional non-proteinaceous  
316 neurotoxin, TTX, within their venom. We hypothesize that the *Hapalochlaena* PSG will  
317 exhibit a loss of redundant proteinaceous toxins due to the presence of TTX.

318           Examination of all PSG-specific genes from the three octopods revealed a  
319 disproportionate number of genes exclusive to *H. maculosa* (Fig 3a). A total of 623

320 genes were exclusive to *H. maculosa* PSG compared to only 230 and 164 exclusive to *O.*  
321 *bimaculoides* and *C. minor* PSGs, respectively. Additionally, we predict that the *H.*  
322 *maculosa* PSG is functionally more diverse based on the number of Pfam families  
323 detected, 532 in total. Comparatively, the PSG genes in *O. bimaculoides* and *C. minor*  
324 are fewer and more specialised. Gene family expansions of serine proteases dominate  
325 expression comprising over 30% of total PSG-specific expression in *C. minor* and 17-  
326 20% in *O. bimaculoides* (Fig 3b). Serine proteases were also among genes whose  
327 expression appears to have shifted between octopod species. Several serine proteases  
328 show specific expression to the PSG of *O. bimaculoides* and *C. minor* while being  
329 expressed in a non-specific pattern among brain, skin, muscle and anterior salivary  
330 gland tissues in *H. maculosa* (Fig 4b). Most notable is the absence of many paralogs in  
331 both *H. maculosa* and *O. bimaculoides* suggesting a lineage-specific expansion of this  
332 cluster in *C. minor*. Fewer serine protease genes can also be observed in *H. maculosa*  
333 (Fig 4c). Similarly, reprotolysin (M12B) exhibits shifting expression in *H. maculosa*,  
334 presumably from the PSG to the branchial heart, and a complete loss of paralogs from  
335 the genome. While the function of this protein has not been assessed in octopus,

336 members of this protein family exhibit anticoagulant properties in snake venom[75–  
337 78].

338 Serine proteases have been previously documented in cephalopod venom and  
339 are prime candidates for conserved toxins in octopods. Cephalopod-specific expansions  
340 have been identified with strong association to the PSG in 11 cephalopods (seven  
341 octopus, two squid and two cuttlefish)[8,13]. All serine proteases identified from the  
342 PSG of these species were found to belong to the cephalopod-specific clade.

343 Functionally, cephalopod venom serine proteases have yet to be assessed. However,  
344 octopod venom has been observed to have strong digestive and hemolytic properties,  
345 which may be in part due to this crucial protein family[79–81]. The reduced number  
346 and expression of serine proteases in *H. maculosa* suggests a change in function of the  
347 PSG for this species. These results support the hypothesis of toxin redundancy in the *H.*  
348 *maculosa* PSG due to the incorporation of tetrodotoxin. Previous proteomic analysis of  
349 the *H. maculosa* PSG revealed high expression of hyaluronidase, which often serves as a  
350 dispersal factor within snake venom, facilitating the spread of toxin while not being  
351 directly toxic to their prey[9,82]. While further investigation is required, the  
352 incorporation of TTX within *H. maculosa* venom may have contributed to a shift in

353 function, with proteins present acting to support the spread of venom and digestion of  
354 tissues.

355

356 **Fig 4. Examination of posterior salivary gland (PSG) gene expression between three octopod**  
357 **genomes. a)** Heatmap of genes expressed specifically in the PSG of *H. maculosa* ( $\tau > 0.8$ ) and their  
358 orthologs in *O. bimaculoides* and *C. minor* lacking specific expression to the PSG ( $\tau < 0.8$ ). Genes with  
359 an ortholog lacking expression are coloured in grey while the absence of an ortholog is white. **b)**  
360 Heatmap of genes expressed specifically in the (PSG) of both *O. bimaculoides* and *C. minor* ( $\tau > 0.8$ )  
361 and their orthologs in *H. maculosa* lacking specific expression to the PSG.

362

### 363 ***TTX resistance of the $Na_v$ channels***

364 To identify the mechanism of TTX resistance in *H. maculosa*, the voltage gated  
365 sodium channel ( $Na_v$ ) sequences were compared between susceptible (human) and  
366 resistant (pufferfish, salamanders and garter snakes) species. TTX binds to the p-loop  
367 regions of sodium channels, inhibiting the flow of sodium ions in neurons, resulting in  
368 paralysis[83,84]. Inhibition of TTX binding has been observed in species which either

369 ingest TTX via prey, such as garter snakes[85], and in those which retain TTX within  
370 their tissues like pufferfish[86].

371 Two  $Na_v$  genes were identified in the *H. maculosa* genome ( $Na_v1$  and  $Na_v2$ ), this  
372 is congruent with the recent identification of two  $Na_v$  isoforms in *H.*  
373 *lunulata*[24](Supplementary Fig 8 & 9). Among cephalopods with sequenced  $Na_v1$   
374 channels, p-loop regions are highly conserved with both DI and DII shared between all  
375 species. The regions DIII and DIV closer to the C-terminal end of the protein in  
376 *Hapalochlaena* sp. contain mutations, which may impact TTX binding and differ  
377 between families and species as follows. Similar to the pufferfish (*Arothron*,  
378 *Canthigaster*, *Takifugu* and *Tetraodon*)[87]and garter snake *Thamnophis couchii*[88], *H.*  
379 *maculosa* Nav1 has a mutation within the third p-loop at site (DIII) from M1406T,  
380 while all other cephalopods have an Ile(I) at this position (Fig 5a). The dumbo octopus  
381 (*Grimpoteuthis*) is the only exception retaining the susceptible M at this site similar to  
382 humans and other non-resistant mammals[83]. Additionally, the fourth p-loop (DIV) in  
383 *H. maculosa* exhibits two substitutions at known TTX binding sites: D1669H and  
384 H1670S. In a previous study a Met to Thr substitution into a TTX sensitive Nav1.4  
385 channel decreased binding affinity to TTX by 15-fold[87]. Likewise, a 10-fold increase

386 in sensitivity was observed from a T1674M substitution in a mite (*Varroa destructor*)  
387 channel VdNav1[28]. However, resistance is often a result of multiple substitutions and  
388 when I1674T/D1967S occur together in VdNav1, resistance is multiplicative resulting  
389 in “super resistant” channels with binding inhibition of 1000-fold. The combination of  
390 M1406T/ D1669H in *H. maculosa* also occurs in the turbellarian flatworm *Bdelloura*  
391 *candida*(BcNav1)[87,89]. While it has yet to be assessed for TTX resistance, the  
392 replacement of Asp in *B. candida* with a neutral amino acid has been predicted to  
393 disrupt TTX binding by preventing formation of a salt bridge or hydrogen bond[89,90].  
394 These three substitutions (M1406T, D1669H and H1670S) in *H. maculosa*, with the  
395 potential to inhibit TTX binding, have also been identified by Geffeney et al[24] in *H.*  
396 *lunulata*. It has yet to be established if these mutations are derived from a shared  
397 ancestor or have occurred independently.

398       While *Hapalochlaena* remains the best documented example of TTX resistance  
399 among cephalopods, other species may contain some level of TTX resistance (e.g.  
400 *Octopus vulgaris*)[91,92]. Saxitoxin (STX) is a similar toxin in structure and function,  
401 and mutations resistant to TTX are often also STX inhibiting[93] *O. vulgaris* has been  
402 observed consuming STX-contaminated bivalves with no negative impacts and as such

403 is believed to be resistant[92]. However, no mutations known to reduce TTX/STX  
404 binding affinity occur in its Nav1 [92,94]. The selective pressure facilitating the  
405 evolution of STX/TTX resistance in these shallow water benthic octopods may be toxic  
406 prey, similar to garter snakes. STX is also known as a paralytic shellfish poison (PSP).  
407 Produced by photosynthetic dinoflagellates and bioaccumulated in bivalves[95], this  
408 toxin contaminates a common octopus food source. Pelagic squids such as the  
409 Humboldt (*D. gigas*) and longfin inshore squid (*D. pealeii*) do not appear to be TTX/STX  
410 resistant; mass strandings of Humboldt squid have been associated with ingestion of  
411 STX-contaminated fish[96]. Likewise, no evidence of resistance was found in the  
412 sodium channel of the dumbo octopus (*Grimpoteuthis*). This species typically inhabits  
413 depths of 2000-5000m and is unlikely to encounter STX-contaminated food  
414 sources[97].

415

416 **Fig 5. Mechanism of tetrodotoxin resistance within the posterior salivary gland of *H. maculosa***  
417 **(PSG) a)** Alignment of voltage gated sodium channel alpha subunits (DI, DII, DIII & DIV) p-loop regions.  
418 Mutations conferring resistance are coloured in green (pufferfish), orange (salamander), purple (clam)  
419 and blue (octopus). Susceptible mutations at the same site are Black and bolded. Sites which may be



420 involved with resistance are in bold. **b)** Schematic of voltage-gated sodium channel (Na<sub>v</sub>) alpha subunits  
421 (DI, DII, DIII and DIV). Each unit is composed of six subunits 1-4 (blue) and 5-6 (yellow). Alternating  
422 extra and intercellular loops are shown in black with the p-loops between subunits 5 and 6 highlighted  
423 in red. Mutations conferring resistance are shown within black circles on p-loops.

424

### 425 ***Microbiome of the PSG***

426 TTX is produced through a wide variety of bacteria, which are common in  
427 marine sediments and have been isolated from organisms such as  
428 pufferfish[25,98,99]. Sequestration of TTX is not exclusive to the blue-ringed octopus  
429 among molluscs. Gastropods such as *Pleurobranchaea maculata*[100] and *Niotha*  
430 *clathrata*[30], as well as some bivalves, are also capable of sequestering TTX[95]. The  
431 commonly held hypothesis for TTX acquisition within *Hapalochlaena* is that it is  
432 bacterial in origin, and is either ingested or endosymbiotic[100,101]. Analysis of a  
433 ribo-depleted RNA sample from the PSG of *H. maculosa* revealed a highly diverse  
434 composition of bacterial genera with Simpson's and Shannon's diversity indices of 4.77  
435 and 0.94, respectively. The dominant phyla were Proteobacteria and Firmicutes,  
436 composing respectively 41% and 22% of overall bacterial species detected (Fig 5a-b).

437 To date, 151 strains of TTX-producing bacteria have been identified from 31 genera. Of  
438 these, 104 are members of Proteobacteria[102]. The genera *Pseudomonas* and *Bacillus*  
439 belonging to the phyla Proteobacteria and Firmicutes, respectively, have been  
440 previously identified in the PSG of *Hapalochlaena* sp (*Octopus maculosus*)[101].  
441 Examination of these bacterial strains revealed TTX production, and extracts injected  
442 into mice proved to be lethal[101]. A more recent study on the bacterial composition  
443 of *H. maculosa* PSG did not identify TTX-producing strains[100]. However, only a small  
444 subset of the many strains identified were tested. Congruent with our findings the  
445 diversity of bacterial genera was high and this may complicate identification of species  
446 responsible for TTX production. The biosynthetic pathway of TTX has yet to be  
447 elucidated, and as a result, only culturable bacterial species can be tested for TTX  
448 production.

449

450 **Fig 6. Assessment of bacteria within the posterior salivary gland of *H. maculosa* (PSG).** a) Bacterial composition at  
451 the phylum level of a *H. maculosa* posterior salivary/venom gland. b) Composition of the largest Phylum,  
452 Protobacteria of a *H. maculosa* posterior salivary/venom gland.

453

454 ***Conclusions***

455           This work describes the genome of a unique TTX bearing mollusc, the southern  
456 blue-ringed octopus (*Hapalochlaena maculosa*). Much of cephalopod evolution is barely  
457 understood due to sparseness of genomic data. Our analysis provides the first glimpse  
458 into genomic changes underlying genome evolution of closely related octopod species.  
459 While the size, heterozygosity and repetitiveness of the blue ring genome is congruent  
460 with previously published octopod genomes, we find similar yet independent  
461 expansions of key neuronal gene families across all three species and show evidence for  
462 the involvement of gene novelty in the evolution of key neuronal, reproductive, and  
463 sensory tissues. The evolution of venom in octopods also differs between species, with  
464 *H. maculosa* showing a reduction in the number and expression of serine proteases in  
465 their venom gland relative to the other octopods in this study. Inclusion of TTX in *H.*  
466 *maculosa* distinguishes this species from related octopods and is believed to impact  
467 toxin recruitment and retention, as the highly potent TTX is sufficient to subdue  
468 common octopod prey without additional toxins.

469

## 470 ***Methods***

### 471 ***Genome sequencing and assembly***

472 DNA was extracted from a single *H. maculosa* female collected at Port Phillip Bay,  
473 Victoria, Australia. Two types of Illumina libraries were constructed, standard paired  
474 end and Illumina mate pairs (Supplementary data 2). Dovetail sequencing, Chicago  
475 libraries improved upon original sequencing resulting in an overall coverage of 71X.  
476 Assembly-stats[103] was used to ascertain the quality of the assembly and relevant  
477 metrics (Supplementary notes 1).

478

#### 479 ***Transcriptome sequencing***

480 The *H. maculosa* transcriptome was generated using 12 tissues (brain, anterior salivary  
481 gland, digestive gland, renal, brachial heart, male reproductive tract, systemic heart,  
482 eyeballs, gills, posterior salivary gland, dorsal mantle and ventral mantle tissue). RNA  
483 was extracted using the Qiagen RNeasy kit. Construction of cDNA libraries was  
484 outsourced to AGRF (Australian Genome Research Facility), Melbourne and conducted  
485 using their TruSeq mRNA Library Prep with polyA selection and unique dual indexing  
486 method. Libraries were constructed using 3 µg of RNA at a concentration of >100  
487 ng/µ L. Each tissue was sequenced on 1/12th of an Illumina HiSeq2000 lane with one  
488 lane used in total.

489

490 ***De novo transcriptome assembly***

491 *De novo* assembly of the *H. maculosa* transcriptome was conducted using sequencing  
492 data from 11 tissues (as listed above) and Trinity v10.11.201 (Trinity,  
493 RRID:SCR\_013048)[104]. Default parameters were used aside from kmer coverage,  
494 which was set to three to account for the large data volume. Protein coding sequences  
495 were identified using Trinotate (Trinotate, RRID:SCR\_018930) [105] and domains  
496 assigned by Interpro v72.0 (InterPro, RRID:SCR\_006695) [106].

497

498 ***Genome annotation***

499 Genes were annotated using a *de novo* predictor supplemented with transcriptomic  
500 evidence. Training models were produced by PASA (PASA, RRID:SCR\_014656)[38]  
501 using a transcriptome composed of 12 tissues (as listed above) and supplied to the *de*  
502 *novo* predictor Augustus (Augustus, RRID:SCR\_008417) [39] along with intron, exon  
503 and repeat hints (generated by repeatmasker). Alternative splicing of gene models was  
504 also predicted using PASA (PASA, RRID:SCR\_014656). Methods used for annotation  
505 have been documented in the git[107].\_Additional genes were predicted by mapping

506 raw expressed reads against the genome. Functional annotation of gene models was  
507 achieved using InterPro v72.0 (InterPro, RRID:SCR\_006695)[106]. Completeness of  
508 genes was assessed using BUSCO v3 Metazoan database (BUSCO,  
509 RRID:SCR\_015008)[40].

510

### 511 ***Heterozygosity***

512 JELLYFISH v2.2.1 (Jellyfish, RRID:SCR\_005491) was used in conjunction with  
513 GenomeScope (GenomeScope, RRID:SCR\_017014)[108] to calculate heterozygosity in  
514 *H. maculosa* using a kmer frequency of 21 (Supplementary table 5).

515

### 516 ***Repetitive and transposable elements***

517 Repetitive and transposable elements were annotated using RepeatModeler v1.0.9  
518 (RepeatScout) (RepeatModeler, RRID:SCR\_015027) and masking performed with  
519 RepeatMasker v4.0.8 (RepeatMasker, RRID:SCR\_012954)[109](Supplementary notes  
520 3.3). Analysis of gene associated TE was conducted by extracting TE within flanking  
521 regions 10K upstream and downstream of genes using Bedtools v2.27.1 (BEDTools,  
522 RRID:SCR\_006646)[110].

523

524 ***Calibration of sequence divergence with respect to time***

525 Divergence times between the molluscan genomes (*Crassostrea gigas*, *Lottia gigantea*,

526 *Aplysia californica*, *Euprymna scolopes*, *Octopus bimaculoides*, *Callistoctopus minor* and

527 *Hapalochlaena maculosa*) and transcriptomes (*Sepia officinalis*, *Idiosepius notoides*,

528 *Octopus kaurna* and *Octopus vulgaris*) was obtained using a mutual best hit (MBH)

529 approach. Bioprojects for each genome used are as follows: *Crassostera gigas*

530 (PRJNA629593 & PRJEB3535), *Lottia gigantea* (PRJNA259762 & PRJNA175706),

531 *Aplysia californica* (PRJNA629593 & PRJNA13635) and (*Euprymna scolopes*

532 PRJNA47095). *Octopus bimaculoides* was obtained from this link [111]. The , *Idiosepius*

533 *notoides* (BioProject: PRJNA302677) transcriptome was sequenced and assembled using

534 the same method previously described for the *H. maculosa* transcriptome. Whole

535 genomes and transcriptomes were BLASTed against *Octopus bimaculoides*. The resulting

536 hits were filtered, and alignments shared between all species extracted. A maximum

537 likelihood phylogeny was generated using RAxML v8.0 (RAxML,

538 RRID:SCR\_006086)[112]. Phylobayes v3.3 (PhyloBayes, RRID:SCR\_006402)[113] was

539 used to calculate divergence times (Supplementary 4.1).

540

541 ***Effective population size (PSMC)***

542 Historical changes in effective population size were estimated using PSMC  
543 implemented in the software MSMC[114,115]. To generate inputs for MSMC we  
544 selected a subset of the reads used for genome assembly corresponding to 38x coverage  
545 of reads from libraries with short (500bp) insert sizes. These were pre-processed  
546 according to GATK best practices; briefly, adapters were marked with Picard 2.2.1,  
547 reads were mapped to the *H. maculosa* genome using bwa mem v 0.7.17 (BWA,  
548 RRID:SCR\_010910)[116] and PCR duplicates identified using Picard v2.2.1. In order to  
549 avoid inaccuracies due to poor coverage or ambiguous read mapping we masked  
550 regions where short reads would be unable to find unique matches using SNPable[117]  
551 and where coverage was more than double or less than half the genome wide average  
552 of 38x. Variant sites were called within unmasked regions and results converted to  
553 MSMC input format using msmc-tools[118] . All data for *H. maculosa* scaffolds of  
554 length greater than 1Mb was then used to generate 100 bootstrap replicates by dividing  
555 data into 500kb chunks and assembling them into 20 chromosomes with 100 chunks  
556 each. We then ran msmc2 on each bootstrap replicate and assembled imported the



557 resulting data into R for plotting. A mutation rate of  $2.4e-9$  per base per year and a  
558 generation time of 1 year were assumed in order to set a timescale in years and convert  
559 coalescence rates to effective population size.

560

### 561 ***Mutation rate***

562 Mutation rate was calculated by extracting orthologous genes from *O. bimaculoides* and  
563 *H. maculosa*. Neutrality was assumed for genes with very low expression ( $> 10$  TMP  
564 across all tissues). Neutral genes were aligned using MAFFT v7.407[119] and codeml  
565 (PAML, RRID:SCR\_014932)[120] was used to calculate substitution metrics (dS). Per  
566 base neutral substitution between lineages was determined using the mean dS value  
567 divided by divergence time (refer to *Calibration of sequence divergence with respect to*  
568 *time*) over the number of generations. As octopus are diploid the rate was divided by  
569 two. Divergence between species was calculated using Phylobayes v3.3 (PhyloBayes,  
570 RRID:SCR\_006402)[113].

571

### 572 ***Quantifying gene expression/ specificity***

573 Gene expression within individual tissues was calculated using Kallisto (kallisto,  
574 RRID:SCR\_016582)[121] for the transcriptomic data sets of *H. maculosa*, *O.*  
575 *bimaculoides* and *C. minor*. Defaults were used and counts were calculated as TPM.  
576 Gene specificity was defined as any gene with a tau value  $> 0.80$ .

577

### 578 ***Gene model expression dynamics***

579 Patterns of gene expression and loss were assessed across octopod genomes at differing  
580 taxonomic/organismal levels. Gene models were classified as lineage-specific, octopod  
581 specific or non-specific (orthologous to a gene outside of octopods). Expression at each  
582 level was determined using whole transcriptomes from all tissues of each species. Genes  
583 with expression within one or more tissues were determined to be expressed, loss of  
584 expression was classified as a gene with a single ortholog in each species, which is  
585 expressed in one or more species and not expressed in the remaining species.

586

### 587 ***Dynamics of PSG gene expression***

588 In order to identify patterns of PSG specific gene expression (losses and shifts) between  
589 the three available octopod genomes, genes with expression specific to the PSG of each

590 species were examined separately. Specific gene expression was defined as a tau value  
591 > 0.8. Orthologous groups were identified between species using OrthoVenn2[122]  
592 and sequences which were identified as lineage-specific were confirmed using BLAST.  
593 Types of expressions were categorized as follows: A loss of expression requires a gene  
594 to be present in all three octopods and expressed in one or more species while having  
595 no detectable expression in at least one species. A shift in expression occurs when an  
596 ortholog present in all species is expressed in different tissues.

597

### 598 ***The role of the Nav in TTX resistance***

599 Sodium channels for the three octopus genomes along with all available in-house  
600 cephalopod transcriptomes were extracted manually using a series of BLAST searches  
601 against the nr database. Annotation was achieved using Interpro v72.0 (InterPro,  
602 RRID:SCR\_006695)[106] and identification and extraction of p-loop regions of the  
603 sodium channel alpha subunit were manually performed. Where sodium channels were  
604 incomplete alignment against related complete channels were used to extract the p-  
605 loop regions. Individual mutations with potential to confer resistance were identified  
606 manually in Geneious v10.1[123].

607

608 ***Microbiome of PSG***

609 A single ribo-depleted RNA sample of *H. maculosa* PSG was examined using the  
610 SAMSA2 pipeline[124] to identify the bacterial composition and corresponding  
611 molecular functions. Two databases were used Subsys and NCBI RefBac. The Krona  
612 package[125] was used to produce visualizations of each dataset.

613

614 **Availability of source code and requirements**

615 Project name: BRO\_annotation

616 Project home page: [https://github.com/blwhitelaw/BRO\\_annotation](https://github.com/blwhitelaw/BRO_annotation)

617 Operating system(s): linux

618 Programming language: Unix/Bash

619 Other requirements: HPC

620 License: GPL-2.0 License

621 Any restrictions to use by non-academics: none

622 RRID: SCR\_019072

623

624 **Availability of supporting data and materials**

625 Genomic and transcriptomic data produced and used in this paper have been made  
626 available in the NCBI BioProject: PRJNA602771 under the following accession  
627 numbers: raw transcriptome (SAMN13930963 - SAMN13930975), genome assembly  
628 (SAMN13906985), raw genome reads (SAMN13906958), gene models  
629 (SAMN13942395). Voucher specimen for the transcriptome is stored at Melbourne  
630 museum. All supporting data and materials are available in the *GigaScience* GigaDB  
631 database [126]. This includes expression data for the transcriptome, raw  
632 transcriptomes reads, gene models, gene annotation gff and assembled genome, as well  
633 as files used in figure generation (i.e. trees, heatmaps).

634

635 **Supplementary Information**

636 Supplementary Notes 1-8, Supplementary Tables 1-8, Supplementary Figs 1-10

637 Supplementary Data 2: Table of genomic Illumina library insert sizes

638

639 **Abbreviations**

640 TTX: Tetrodotoxin, STX: Saxitoxin, PSG: Posterior Salivary Gland, CHGN:Chondroitin  
641 N-acetylgalactosaminyltransferase, C2H2(Cys2-His2) zinc finger, Cornifin SPRR:Small  
642 Proline-Rich Proteins, LINE: Long Interspersed Nuclear Element, SINE: Short  
643 Interspersed Nuclear Element, Mya: Million Years Ago, BUSCO: Benchmarking  
644 Universal Single-Copy Orthologs, PSMC: *Pairwise Sequentially Markovian Coalescent* and  
645 MSMC:multiple sequentially Markovian coalescent

646

#### 647 **Ethics declaration**

648 Animal Ethics Approval

649 Field collection of fishes, cephalopods (nautilus, squids, cuttlefishes and octopuses}  
650 and decapod crustaceans (crabs, lobsters, crayfishes and their allies) in for Museum  
651 Victoria” (Animal Ethics Committee: Museums Victoria; AEC Approval Number: 10006)

652

#### 653 **Competing interests**

654 Authors have no conflicts/competing interests to declare.

655

656 **Acknowledgements**

657 We thank Dr Mark Norman and Colin Silvey for aiding Dr Julian Finn in collection of  
658 the two blue-ringed octopus specimens. We thank Jacqui Stuart for her brilliant  
659 illustrations and work on Figure beautification. This work was supported by an  
660 Australian Biological Resources Study (ABRS) grant (ref:RF211-41). O. Simakov was  
661 supported by the Austrian Science Fund (FWF) grant P30686-B29.

662

663 **References**

664

- 665 1. Ritschard EA, Whitelaw B, Albertin CB, Cooke IR, Strugnell JM, Simakov O.  
666 Coupled Genomic Evolutionary Histories as Signatures of Organismal Innovations  
667 in Cephalopods. *BioEssays*. 2019;
- 668 2. Tanner AR, Fuchs D, Winkelmann IE, Gilbert MTP, Pankey MS, Ribeiro ÂM, et al.  
669 Molecular clocks indicate turnover and diversification of modern coleoid  
670 cephalopods during the Mesozoic Marine Revolution. *Proc R Soc B Biol Sci*.  
671 2017;284(1850):2016–818.
- 672 3. Jereb Roper, C. F. E., Norman, M. D., and Finn, J. K. P. Cephalopods of the  
673 world. An annotated and illustrated catalogue of cephalopod species known to  
674 date,” in *Octopods and Vampire Squids*, Vol. 3,. Rome FAO. 2014;
- 675 4. Graziadei PPC, Gagne HT. Sensory innervation in the rim of the octopus sucker. *J*  
676 *Morphol*. 1976;150(3):639–79.
- 677 5. Froesch D. Projection of chromatophore nerves on the body surface of *Octopus*  
678 *vulgaris*. *Mar Biol*. 1973;19(2):153–5.
- 679 6. Budelmann BU. The cephalopod nervous system: what evolution has made of the  
680 molluscan design. In: *The nervous systems of invertebrates: An evolutionary and*  
681 *comparative approach*. Springer; 1995. p. 115–38.

- 682 7. Gray EG, Young JZ. Electron microscopy of synaptic structure of Octopus brain. *J*  
683 *Cell Biol.* 1964;21(1):87–103.
- 684 8. Fingerhut LCHW, Strugnell JM, Faou P, Labiaga ÁR, Zhang J, Cooke IR. Shotgun  
685 proteomics analysis of saliva and salivary gland tissue from the common octopus  
686 *Octopus vulgaris*. *J Proteome Res.* 2018;17(11):3866–76.
- 687 9. Whitelaw BL, Cooke IR, Finn J, Zenger K, Strugnell JM. The evolution and origin  
688 of tetrodotoxin acquisition in the blue-ringed octopus (genus *Hapalochlaena*).  
689 *Aquat Toxicol.* 2019;206:114–22.
- 690 10. Cooke IR, Whitelaw B, Norman M, Caruana N, Strugnell JM. Toxicity in  
691 cephalopods. *Evol Venom Anim Their Toxins.* 2015;1–15.
- 692 11. Whitelaw BL, Strugnell JM, Faou P, Da Fonseca RR, Hall NE, Norman M, et al.  
693 Combined Transcriptomic and Proteomic Analysis of the Posterior Salivary Gland  
694 from the Southern Blue-Ringed Octopus and the Southern Sand Octopus. *J*  
695 *Proteome Res.* 2016;15(9):3284–97.
- 696 12. Fry BG, Roelants K, Norman JA. Tentacles of venom: toxic protein convergence in  
697 the Kingdom Animalia. *J Mol Evol.* 2009;68(4):311–21.
- 698 13. Ruder T, Sunagar K, Undheim EAB, Ali SA, Wai T-C, Low DHW, et al. Molecular  
699 phylogeny and evolution of the proteins encoded by coleoid (cuttlefish, octopus,  
700 and squid) posterior venom glands. *J Mol Evol.* 2013;76(4):192–204.
- 701 14. Fry BG, Winter K, Norman JA, Roelants K, Nabuurs RJA, Van Osch MJP, et al.  
702 Functional and structural diversification of the anguimorpha lizard venom  
703 system. *Mol Cell Proteomics.* 2010;9(11):2369–90.
- 704 15. Hendon RA, Tu AT. Biochemical Characterization of the Lizard Toxin Gilatoxin.  
705 *Biochemistry.* 1981;20(12):3517–22.
- 706 16. Matsui T, Fujimura Y, Titani K. Snake venom proteases affecting hemostasis and  
707 thrombosis. *Biochimica et Biophysica Acta - Protein Structure and Molecular*  
708 *Enzymology.* 2000. p. 146–56.
- 709 17. Mitreva M, Papenfuss AT, Whittington CM, Locke DP, Mardis E, Wilson RK, et al.  
710 Novel venom gene discovery in the platypus. *Genome Biol.* 2010;11:1–13.
- 711 18. Choo YM, Lee KS, Yoon HJ, Qiu Y, Wan H, Sohn MR, et al. Antifibrinolytic role  
712 of a bee venom serine protease inhibitor that acts as a plasmin inhibitor. *PLoS*  
713 *One.* 2012;7(2):e32269.
- 714 19. Veiga SS, Da Silveira RB, Dreyfuss JL, Haoach J, Pereira AM, Mangili OC, et al.



- 715 Identification of high molecular weight serine-proteases in *Loxosceles intermedia*  
716 (brown spider) venom. *Toxicon*. 2000;38(6):825–39.
- 717 20. Modica MV, Lombardo F, Franchini P, Oliverio M. The venomous cocktail of the  
718 vampire snail *Colubraria reticulata* (Mollusca, Gastropoda). *BMC Genomics*.  
719 2015;16(1):1–21.
- 720 21. von Reumont BM, Undheim EAB, Jaus RT, Jenner RA. Venomics of remipede  
721 crustaceans reveals novel peptide diversity and illuminates the venom’s  
722 biological role. *Toxins (Basel)*. 2017;9(8):234.
- 723 22. Jaimes-Becerra A, Chung R, Morandini AC, Weston AJ, Padilla G, Gacesa R, et al.  
724 Comparative proteomics reveals recruitment patterns of some protein families in  
725 the venoms of Cnidaria. *Toxicon*. 2017;137:19–26.
- 726 23. Crone HD, Leake B, Jarvis MW, Freeman SE. On the nature of “Maculotoxin”, a  
727 toxin from the blue-ringed octopus (*Hapalochlaena maculosa*). *Toxicon*.  
728 1976;14(6):423–6.
- 729 24. Geffeney SL, Williams BL, Rosenthal JJC, Birk MA, Felkins J, Wisell CM, et al.  
730 Convergent and parallel evolution in a voltage-gated sodium channel underlies  
731 TTX-resistance in the Greater Blue-ringed Octopus: *Hapalochlaena lunulata*.  
732 *Toxicon*. 2019;170:77–84.
- 733 25. Wu Z, Yang Y, Xie L, Xia G, Hu J, Wang S, et al. Toxicity and distribution of  
734 tetrodotoxin-producing bacteria in puffer fish *Fugu rubripes* collected from the  
735 Bohai Sea of China. *Toxicon*. 2005;46(4):471–6.
- 736 26. Tsuruda K, Arakawa O, Kawatsu K, Hamano Y, Takatani T, Noguchi T. Secretory  
737 glands of tetrodotoxin in the skin of the Japanese newt *Cynops pyrrhogaster*.  
738 *Toxicon*. 2002;40(2):131–6.
- 739 27. Wakely JF, Fuhrman GJ, Fuhrman FA, Fischer HG, Mosher HS. The occurrence of  
740 tetrodotoxin (tarichatoxin) in Amphibia and the distribution of the toxin in the  
741 organs of newts (*Taricha*). *Toxicon*. 1966;3(3):195–203.
- 742 28. Du Y, Nomura Y, Liu Z, Huang ZY, Dong K. Functional expression of an arachnid  
743 sodium channel reveals residues responsible for tetrodotoxin resistance in  
744 invertebrate sodium channels. *J Biol Chem*. 2009;284(49):33869–75.
- 745 29. McGlothlin JW, Chuckalovcak JP, Janes DE, Edwards S V, Feldman CR, Brodie Jr  
746 ED, et al. Parallel evolution of tetrodotoxin resistance in three voltage-gated  
747 sodium channel genes in the garter snake *Thamnophis sirtalis*. *Mol Biol Evol*.

- 748 2014;31(11):2836–46.
- 749 30. Cheng CA, Hwang DF, Tsai YH, Chen HC, Jeng SS, Noguchi T, et al. Microflora  
750 and tetrodotoxin-producing bacteria in a gastropod, *Niotha clathrata*. *Food Chem*  
751 *Toxicol.* 1995;33(11):929–34.
- 752 31. Williams BL, Caldwell RL. Intra-organismal distribution of tetrodotoxin in two  
753 species of blue-ringed octopuses (*Hapalochlaena fasciata* and *H. lunulata*).  
754 *Toxicon.* 2009;54(3):345–53.
- 755 32. Yotsu-Yamashita M, Mebs D, Flachsenberger W. Distribution of tetrodotoxin in  
756 the body of the blue-ringed octopus (*Hapalochlaena maculosa*). *Toxicon.*  
757 2007;49(3):410–2.
- 758 33. Mäthger LM, Bell GRR, Kuzirian AM, Allen JJ, Hanlon RT. How does the blue-  
759 ringed octopus (*Hapalochlaena lunulata*) flash its blue rings? *J Exp Biol.*  
760 2012;215(21):3752–7.
- 761 34. Williams BL, Stark MR, Caldwell RL. Microdistribution of tetrodotoxin in two  
762 species of blue-ringed octopuses (*Hapalochlaena lunulata* and *Hapalochlaena*  
763 *fasciata*) detected by fluorescent immunolabeling. *Toxicon.* 2012;60(7):1307–13.
- 764 35. Savage IVE, Howden MEH. Hapalotoxin, a second lethal toxin from the octopus  
765 *Hapalochlaena maculosa*. *Toxicon.* 1977;15(5):463–6.
- 766 36. Kanda A, Iwakoshi-Ukena E, Takuwa-Kuroda K, Minakata H. Isolation and  
767 characterization of novel tachykinins from the posterior salivary gland of the  
768 common octopus *Octopus vulgaris*. *Peptides.* 2003;24(1):35–43.
- 769 37. Ruder T, Ali SA, Ormerod K, Brust A, Roymanchadi M-L, Ventura S, et al.  
770 Functional characterization on invertebrate and vertebrate tissues of tachykinin  
771 peptides from octopus venoms. *Peptides.* 2013;47:71–6.
- 772 38. Haas BJ, Delcher AL, Mount SM, Wortman JR, Smith Jr RK, Hannick LI, et al.  
773 Improving the *Arabidopsis* genome annotation using maximal transcript  
774 alignment assemblies. *Nucleic Acids Res.* 2003;31(19):5654–66.
- 775 39. Stanke M. Gene prediction with a hidden Markov model. University of Göttingen;  
776 2004.
- 777 40. Waterhouse RM, Seppey M, Simão FA, Manni M, Ioannidis P, Klioutchnikov G, et  
778 al. BUSCO applications from quality assessments to gene prediction and  
779 phylogenomics. *Mol Biol Evol.* 2017;35(3):543–8.
- 780 41. Zarrella I, Herten K, Maes GE, Tai S, Yang M, Seuntjens E, et al. The survey and

- 781 reference assisted assembly of the *Octopus vulgaris* genome. *Sci data*.  
782 2019;6(1):13.
- 783 42. Albertin CB, Simakov O, Mitros T, Wang ZY, Pungor JR, Edsinger-Gonzales E, et  
784 al. The octopus genome and the evolution of cephalopod neural and  
785 morphological novelties. *Nature* [Internet]. 2015;524(7564):220–4. Available  
786 from: <https://dx.doi.org/10.1038/nature14668>
- 787 43. Cai H, Li Q, Fang X, Li J, Curtis NE, Altenburger A, et al. A draft genome  
788 assembly of the solar-powered sea slug *Elysia chlorotica*. *Sci data*.  
789 2019;6:190022.
- 790 44. Liu C, Zhang Y, Ren Y, Wang H, Li S, Jiang F, et al. The genome of the golden  
791 apple snail *Pomacea canaliculata* provides insight into stress tolerance and  
792 invasive adaptation. *Gigascience*. 2018;7(9):giy101.
- 793 45. Du X, Fan G, Jiao Y, Zhang H, Guo X, Huang R, et al. The pearl oyster *Pinctada*  
794 *fucata martensii* genome and multi-omic analyses provide insights into  
795 biomineralization. *Gigascience*. 2017;6(8):gix059.
- 796 46. Powell D, Subramanian S, Suwansa-ard S, Zhao M, O'Connor W, Raftos D, et al.  
797 The genome of the oyster *Saccostrea* offers insight into the environmental  
798 resilience of bivalves. *DNA Res*. 2018;25(6):655–65.
- 799 47. Sun J, Zhang Y, Xu T, Zhang Y, Mu H, Zhang Y, et al. Adaptation to deep-sea  
800 chemosynthetic environments as revealed by mussel genomes. *Nat Ecol Evol*.  
801 2017;1(5):121.
- 802 48. Uliano-Silva M, Dondero F, Dan Otto T, Costa I, Lima NCB, Americo JA, et al. A  
803 hybrid-hierarchical genome assembly strategy to sequence the invasive golden  
804 mussel, *Limnoperna fortunei*. *Gigascience*. 2017;7(2):gix128.
- 805 49. Zhang G, Fang X, Guo X, Li L, Luo R, Xu F, et al. The oyster genome reveals stress  
806 adaptation and complexity of shell formation. *Nature*. 2012;490(7418):49.
- 807 50. Jiao W, Fu X, Dou J, Li H, Su H, Mao J, et al. High-resolution linkage and  
808 quantitative trait locus mapping aided by genome survey sequencing: building up  
809 an integrative genomic framework for a bivalve mollusc. *DNA Res*.  
810 2013;21(1):85–101.
- 811 51. Garton DW, Haag WR. Heterozygosity, shell length and metabolism in the  
812 European mussel, *Dreissena polymorpha*, from a recently established population  
813 in Lake Erie. *Comp Biochem Physiol Part A Physiol*. 1991;99(1–2):45–8.

- 814 52. Simmons MJ, Crow JF. Mutations affecting fitness in *Drosophila* populations.  
815 *Annu Rev Genet.* 1977;11(1):49–78.
- 816 53. Kumar S, Subramanian S. Mutation rates in mammalian genomes. *Proc Natl Acad*  
817 *Sci.* 2002;99(2):803–8.
- 818 54. Hayward BW, Kawagata S, Grenfell HR, Sabaa AT, O’Neill T. Last global  
819 extinction in the deep sea during the mid-Pleistocene climate transition.  
820 *Paleoceanogr Paleoclimatology.* 2007;22(3).
- 821 55. Hofreiter M, Stewart J. Ecological change, range fluctuations and population  
822 dynamics during the Pleistocene. *Curr Biol.* 2009;19(14):R584–94.
- 823 56. Reynolds T V, Matthee CA, Von Der Heyden S. The influence of Pleistocene  
824 climatic changes and ocean currents on the phylogeography of the southern  
825 African barnacle, *Tetraclita serrata* (Thoracica; Cirripedia). *PLoS One.*  
826 2014;9(7):e102115.
- 827 57. Huber CD, DeGiorgio M, Hellmann I, Nielsen R. Detecting recent selective sweeps  
828 while controlling for mutation rate and background selection. *Mol Ecol.*  
829 2016;25(1):142–56.
- 830 58. Mao Y, Economo EP, Satoh N. The roles of introgression and climate change in  
831 the rise to dominance of *Acropora* Corals. *Curr Biol.* 2018;28(21):3373-3382. e5.
- 832 59. Kim B-M, Amores A, Kang S, Ahn D-H, Kim J-H, Kim I-C, et al. Antarctic blackfin  
833 icefish genome reveals adaptations to extreme environments. *Nat Ecol Evol.*  
834 2019;3(3):469.
- 835 60. Guzik MT, Norman MD, Crozier RH. Molecular phylogeny of the benthic shallow-  
836 water octopuses (Cephalopoda: Octopodinae). *Mol Phylogenet Evol* [Internet].  
837 2005;37(1):235–48. Available from:  
838 <https://dx.doi.org/10.1016/j.ympev.2005.05.009>
- 839 61. Strugnell J, Jackson J, Drummond AJ, Cooper A. Divergence time estimates for  
840 major cephalopod groups: evidence from multiple genes. *Cladistics.*  
841 2006;22(1):89–96.
- 842 62. Strugnell JM, Rogers AD, Prodöhl PA, Collins MA, Allcock AL. The thermohaline  
843 expressway: the Southern Ocean as a centre of origin for deep-sea octopuses.  
844 *Cladistics.* 2008;24(6):853–60.
- 845 63. Lindgren AR, Anderson FE. Assessing the utility of transcriptome data for  
846 inferring phylogenetic relationships among coleoid cephalopods. *Mol Phylogenet*

- 847 Evol. 2018;118:330–42.
- 848 64. Styfhals R, Seuntjens E, Simakov O, Sanges R, Fiorito G. In silico Identification  
849 and Expression of Protocadherin Gene Family in *Octopus vulgaris*. *Frontiers in*  
850 *Physiology*. 2019. p. 1905.
- 851 65. Zipursky SL, Sanes JR. Chemoaffinity revisited: dscams, protocadherins, and  
852 neural circuit assembly. *Cell*. 2010;143(3):343–53.
- 853 66. Tepass U, Truong K, Godt D, Ikura M, Peifer M. Cadherins in embryonic and  
854 neural morphogenesis. *Nat Rev Mol Cell Biol*. 2000;1(2):91.
- 855 67. Peek SL, Mah KM, Weiner JA. Regulation of neural circuit formation by  
856 protocadherins. *Cellular and Molecular Life Sciences*. 2017. p. 4133–57.
- 857 68. De Wit J, Ghosh A. Specification of synaptic connectivity by cell surface  
858 interactions. *Nat Rev Neurosci*. 2016;1:4.
- 859 69. Layden MJ, Meyer NP, Pang K, Seaver EC, Martindale MQ. Expression and  
860 phylogenetic analysis of the *zic* gene family in the evolution and development of  
861 metazoans. *Evodevo*. 2010;1(1):12.
- 862 70. Liu H, Chang L-H, Sun Y, Lu X, Stubbs L. Deep vertebrate roots for mammalian  
863 zinc finger transcription factor subfamilies. *Genome Biol Evol*. 2014;6(3):510–25.
- 864 71. Young JZ. The number and sizes of nerve cells in *Octopus*. In: *Proceedings of the*  
865 *Zoological Society of London*. Wiley Online Library; 1963. p. 229–54.
- 866 72. Belcaid M, Casaburi G, McAnulty SJ, Schmidbaur H, Suria AM, Moriano-  
867 Gutierrez S, et al. Symbiotic organs shaped by distinct modes of genome  
868 evolution in cephalopods. *Proc Natl Acad Sci [Internet]*. 2019;116(8):3030–5.  
869 Available from: <https://dx.doi.org/10.1073/pnas.1817322116>
- 870 73. Kim B-M, Kang S, Ahn D-H, Jung S-H, Rhee H, Yoo JS, et al. The genome of  
871 common long-arm octopus *Octopus minor*. *Gigascience*. 2018;7(11):giy119.
- 872 74. Kapitonov V V, Jurka J. Rolling-circle transposons in eukaryotes. *Proc Natl Acad*  
873 *Sci*. 2001;98(15):8714–9.
- 874 75. Oulion B, Dobson JS, Zdenek CN, Arbuckle K, Lister C, Coimbra FCP, et al. Factor  
875 X activating *Atractaspis* snake venoms and the relative coagulotoxicity  
876 neutralising efficacy of African antivenoms. *Toxicol Lett*. 2018;15:119–28.
- 877 76. Rogalski A, Soerensen C, op den Brouw B, Lister C, Dashevsky D, Arbuckle K, et  
878 al. Differential procoagulant effects of saw-scaled viper (*Serpentes: Viperidae:*  
879 *Echis*) snake venoms on human plasma and the narrow taxonomic ranges of

- 880 antivenom efficacies. *Toxicol Lett.* 2017;280:159–70.  
881 <http://www.sciencedirect.com/science/article/pii/S0378427417312675>
- 882 77. Sousa LF, Zdenek CN, Dobson JS, den Brouw B op, Coimbra FCP, Gillett A, et al.  
883 Coagulotoxicity of Bothrops (lancehead pit-vipers) venoms from Brazil:  
884 Differential biochemistry and antivenom efficacy resulting from prey-driven  
885 venom variation. *Toxins (Basel)*. 2018;
- 886 78. Fox JW, Serrano SMT. Structural considerations of the snake venom  
887 metalloproteinases, key members of the M12 reprolysin family of  
888 metalloproteinases. *Toxicon*. 2005;45(8):969–85.
- 889 79. Grisley MS, Boyle PR. Bioassay and proteolytic activity of digestive enzymes from  
890 octopus saliva. *Comp Biochem Physiol Part B Comp Biochem*. 1987;88(4):1117–  
891 23.
- 892 80. Key LN, Boyle PR, Jaspars M. Novel activities of saliva from the octopus *Eledone*  
893 *cirrhusa* (Mollusca; Cephalopoda). *Toxicon*. 2002;40(6):677–83.
- 894 81. McDonald NM, Cottrell GA. Purification and mode of action of toxin from  
895 *Eledone cirrosa*. *Comp Gen Pharmacol*. 1972;3(10):243–8.
- 896 82. Bordon KCF, Perino MG, Giglio JR, Arantes EC. Isolation, enzymatic  
897 characterization and antiedematogenic activity of the first reported rattlesnake  
898 hyaluronidase from *Crotalus durissus terrificus* venom. *Biochimie*.  
899 2012;94(12):2740–8.
- 900 83. Frank HY, Catterall WA. Overview of the voltage-gated sodium channel family.  
901 *Genome Biol*. 2003;4(3):207.
- 902 84. How C-K, Chern C-H, Huang Y-C, Wang L-M, Lee C-H. Tetrodotoxin poisoning.  
903 *Am J Emerg Med*. 2003;21(1):51–4.
- 904 85. Brodie III ED, Brodie Jr ED. Tetrodotoxin resistance in garter snakes: an  
905 evolutionary response of predators to dangerous prey. *Evolution (N Y)*.  
906 1990;44(3):651–9.
- 907 86. Nakamura M, Yasumoto T. Tetrodotoxin derivatives in puffer fish. *Toxicon*.  
908 1985;23(2):271–6.
- 909 87. Jost MC, Hillis DM, Lu Y, Kyle JW, Fozzard HA, Zakon HH. Toxin-resistant  
910 sodium channels: parallel adaptive evolution across a complete gene family. *Mol*  
911 *Biol Evol*. 2008;25(6):1016–24.
- 912 88. Feldman CR, Brodie ED, Pfrender ME. Constraint shapes convergence in

- 913 tetrodotoxin-resistant sodium channels of snakes. *Proc Natl Acad Sci.*  
914 2012;109(12):4556–61.
- 915 89. Jeziorski MC, Greenberg RM, Anderson PA V. Cloning of a putative voltage-gated  
916 sodium channel from the turbellarian flatworm *Bdelloura candida*. *Parasitology.*  
917 1997;115(3):289–96.
- 918 90. Shen H, Li Z, Jiang Y, Pan X, Wu J, Cristofori-Armstrong B, et al. Structural basis  
919 for the modulation of voltage-gated sodium channels by animal toxins. *Science*  
920 (80- ). 2018;362:6412.
- 921 91. Flachsenberger W, Kerr DIB. Lack of effect of tetrodotoxin and of an extract from  
922 the posterior salivary gland of the blue-ringed octopus following injection into  
923 the octopus and following application to its brachial nerve. *Toxicon.*  
924 1985;23(6):997–9.
- 925 92. Lopes VM, Baptista M, Repolho T, Rosa R, Costa PR. Uptake, transfer and  
926 elimination kinetics of paralytic shellfish toxins in common octopus (*Octopus*  
927 *vulgaris*). *Aquat Toxicol.* 2014;146:205–11.
- 928 93. Ulbricht W, Wagner H, Schmidtmayer J. Kinetics of TTX-STX Block of Sodium  
929 Channels. *Ann N Y Acad Sci.* 1986;479(1):68–83.
- 930 94. Monteiro A, Costa PR. Distribution and selective elimination of paralytic shellfish  
931 toxins in different tissues of *Octopus vulgaris*. *Harmful Algae.* 2011;10(6):732–7.
- 932 95. Li S-C, Wang W-X, Hsieh D. Feeding and absorption of the toxic dinoflagellate  
933 *Alexandriumtamarense* by two marine bivalves from the South China Sea. *Mar*  
934 *Biol.* 2001;139(4):617–24.
- 935 96. Braid HE, Deeds J, DeGrasse SL, Wilson JJ, Osborne J, Hanner RH. Preying on  
936 commercial fisheries and accumulating paralytic shellfish toxins: a dietary  
937 analysis of invasive *Dosidicus gigas* (Cephalopoda Ommastrephidae) stranded in  
938 Pacific Canada. *Mar Biol.* 2012;159(1):25–31.
- 939 97. Shea EK, Ziegler A, Faber C, Shank TM. Dumbo octopod hatchling provides  
940 insight into early cirrate life cycle. *Curr Biol.* 2018;28(4):R144–5.
- 941 98. Lee M-J, Jeong D-Y, Kim W-S, Kim H-D, Kim C-H, Park W-W, et al. A  
942 tetrodotoxin-producing *Vibrio* strain, LM-1, from the puffer fish *Fugu*  
943 *vermicularis radiatus*. *Appl Environ Microbiol.* 2000;66(4):1698–701.
- 944 99. Yotsu M, Yamazaki T, Meguro Y, Endo A, Murata M, Naoki H, et al. Production  
945 of tetrodotoxin and its derivatives by *Pseudomonas* sp. isolated from the skin of a

946 pufferfish. *Toxicon*. 1987;25(2):225–8.

947 100. Chau R, Kalaitzis J, Wood S, Neilan B. Diversity and biosynthetic potential of  
 948 culturable microbes associated with toxic marine animals. *Mar Drugs*.  
 949 2013;11(8):2695–712.

950 101. Hwang DF, Arakawa O, Saito T, Noguchi T, Simidu U, Tsukamoto K, et al.  
 951 Tetrodotoxin-producing bacteria from the blue-ringed octopus *Octopus*  
 952 *maculosus*. *Mar Biol*. 1989;100(3):327–32.

953 102. Magarlamov T, Melnikova D, Chernyshev A. Tetrodotoxin-producing bacteria:  
 954 Detection, distribution and migration of the toxin in aquatic systems. *Toxins*  
 955 (Basel). 2017;9(5):166.

956 103. assembly-stats. <https://github.com/sanger-pathogens/assembly-stats>. Accessed 29  
 957 Sep 2020

958 104. Grabherr MG, Haas BJ, Yassour M, Levin JZ, Thompson DA, Amit I, et al. Full-  
 959 length transcriptome assembly from RNA-Seq data without a reference genome.  
 960 *Nat Biotechnol*. 2011;29(7):644–52.

961 105. Bryant DM, Johnson K, DiTommaso T, Tickle T, Couger MB, Payzin-Dogru D, et  
 962 al. A tissue-mapped axolotl de novo transcriptome enables identification of limb  
 963 regeneration factors. *Cell Rep*. 2017;18(3):762–76.

964 106. Jones P, Binns D, Chang H-Y, Fraser M, Li W, McAnulla C, et al. InterProScan 5:  
 965 genome-scale protein function classification. *Bioinformatics*. 2014;30(9):1236–  
 966 40.

967 107. BRO\_annotation. [https://github.com/blwhitelaw/BRO\\_annotation](https://github.com/blwhitelaw/BRO_annotation). Accessed 29  
 968 Sep 2020

969 108. Vurture GW, Sedlazeck FJ, Nattestad M, Underwood CJ, Fang H, Gurtowski J, et  
 970 al. GenomeScope: fast reference-free genome profiling from short reads.  
 971 *Bioinformatics*. 2017;33(14):2202–4.

972 109. Smit Hubley, R & Green, P. AFA. RepeatMasker Open-4.0.

973 110. Quinlan AR, Hall IM. BEDTools: a flexible suite of utilities for comparing  
 974 genomic features. *Bioinformatics*. 2010;26(6):841–2.

975 111. *Octopus bimaculoides* genome files.  
 976 [http://octopus.unit.oist.jp/OCTDATA/BASIC/Metazome/Obimaculoides\\_280.fa.g](http://octopus.unit.oist.jp/OCTDATA/BASIC/Metazome/Obimaculoides_280.fa.gz)  
 977 [z](http://octopus.unit.oist.jp/OCTDATA/BASIC/Metazome/Obimaculoides_280.fa.gz). Accessed 29 Sep 2020

978 112. Stamatakis A. RAxML-VI-HPC: maximum likelihood-based phylogenetic analyses



979 with thousands of taxa and mixed models. *Bioinformatics*. 2006;22(21):2688–90.

980 113. Guindon S, Gascuel O. A simple, fast, and accurate algorithm to estimate large  
981 phylogenies by maximum likelihood. *Syst Biol*. 2003;52(5):696–704.

982 114. Li H, Durbin R. Inference of human population history from whole genome  
983 sequence of a single individual. *Nature*. 2012;475(7357):493.

984 115. Schiffels S, Durbin R. Inferring human population size and separation history  
985 from multiple genome sequences. *Nat Genet*. 2014;46(8):919.

986 116. Li H, Durbin R. Fast and accurate short read alignment with Burrows--Wheeler  
987 transform. *bioinformatics*. 2009;25(14):1754–60.

988 117. SNPable. <http://lh3lh3.users.sourceforge.net/snpage.shtml>. Accessed 29 Sep  
989 2020

990 118. msmc-tools. <https://github.com/stschiff/msmc-tools>. Accessed 29 Sep 2020

991 119. Rozewicki J, Li S, Amada KM, Standley DM, Katoh K. MAFFT-DASH: integrated  
992 protein sequence and structural alignment. *Nucleic Acids Res*. 2019;47(W1):W5–  
993 10.

994 120. Adachi J, Hasegawa M. MOLPHY version 2.3: programs for molecular  
995 phylogenetics based on maximum likelihood. Institute of Statistical Mathematics  
996 Tokyo; 1996.

997 121. Bray NL, Pimentel H, Melsted P, Pachter L. Near-optimal probabilistic RNA-seq  
998 quantification. *Nat Biotechnol*. 2016;34(5):525–7.

999 122. Xu L, Dong Z, Fang L, Luo Y, Wei Z, Guo H, et al. OrthoVenn2: a web server for  
1000 whole-genome comparison and annotation of orthologous clusters across multiple  
1001 species. *Nucleic Acids Res*. 2019;47(W1):W52–8.

1002 123. Geneious v10.1.  
1003 [https://assets.geneious.com/documentation/geneious/release\\_notes.html#v10.1](https://assets.geneious.com/documentation/geneious/release_notes.html#v10.1)  
1004 Accessed 29 Sep 2020

1005 124. Westreich ST, Korf I, Mills DA, Lemay DG. SAMSA: a comprehensive  
1006 metatranscriptome analysis pipeline. *BMC Bioinformatics*. 2016;17(1):399.

1007 125. Ondov BD, Bergman NH, Phillippy AM. Interactive metagenomic visualization in  
1008 a Web browser. *BMC Bioinformatics*. 2011;12(1):385.

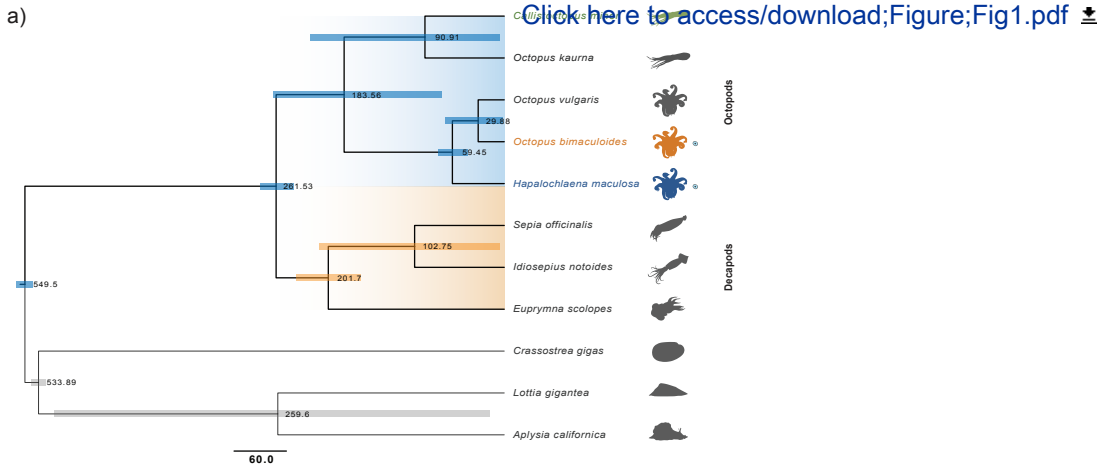
1009 126. Whitelaw BL; Cooke IR; Finn J; da Fonseca RR; Ritschard EA; Gilbert MTP;  
1010 Simakov O; Strugnell JM. Supporting data for "Adaptive venom evolution and  
1011 toxicity in octopods is driven by extensive novel gene formation, expansion and

1012 loss" *GigaScience* Database 2020. <http://dx.doi.org/10.5524/100793>

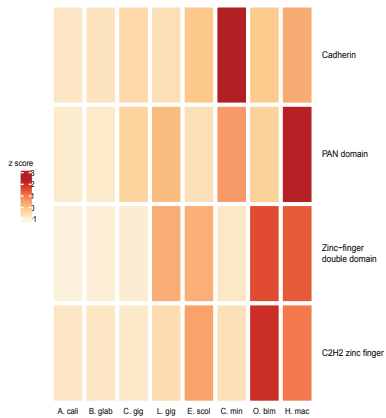
1013

1014

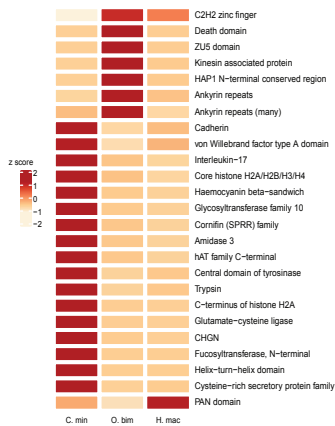
Figure 1

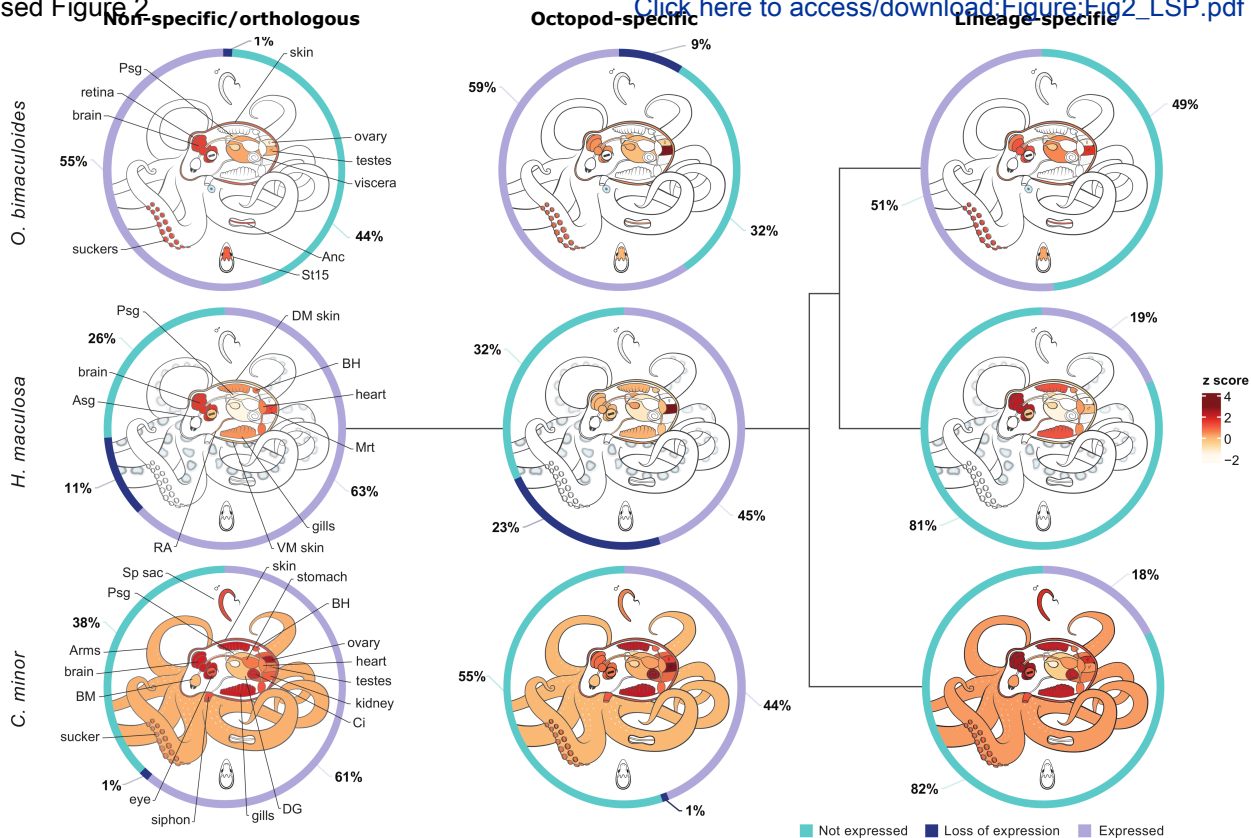


b)

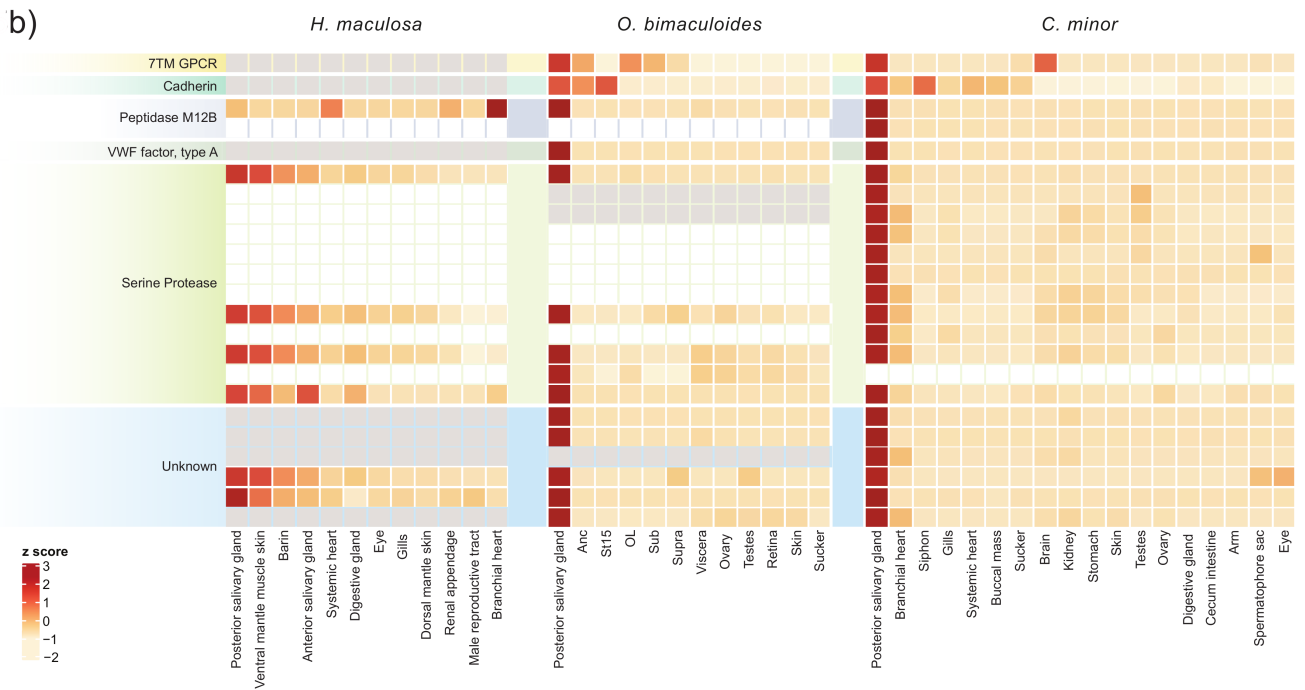


c)
















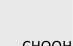






# Revised Figure 5

Click here to access/download;Figure;Fig5PTR\_Au

consensus	<b>DI</b> DYWEN	<b>DII</b> EWIES	<b>DIII</b> RGWXL	<b>DIV</b> RGWDG	
<i>Mya arenaria</i>	-----	--- <u>D</u> ---	---I-	-----	
<i>Crassostrea gigas</i>	F-----	---Q-	---IE	-----	
<i>Mizuhopecten yessoensis</i>	-----	-----	--- <u>T</u> V	---S	
<i>Lottia gigantea</i>	---S-	-----	---V-	-----	
<i>Aplysia californica</i>	F--S-	-----	---I-	---SD	
<i>Euprymna scolopes</i>	-----	-----	---IN	-----	
<i>Doryteuthis pealeii</i>	-----	-----	---IN	-----	
<i>Doryteuthis opalescens</i>	-----	-----	---IN	-----	
<i>Dosidicus gigas</i>	-----	-----	---IN	-----	
<i>Grimpoteuthis</i>	-----	-----	---M-	-----	
<i>Callistoctopus minor</i>	-----	-----	-----	-----	
<i>Octopus bimaculoides</i>	-----	-----	---I-	-----	
<i>Octopus vulgaris</i>	-----	-----	---I-	-----	
<i>Hapalochlaena maculosa</i>	-----	-----	--- <u>T</u> E	--- <u>HS</u> ☠	
<i>Hapalochlaena lunulata</i>	-----	-----	--- <u>T</u> E	--- <u>HS</u> ☠	
<i>Taricha granulosa</i>	-----	---T	--- <u>T</u> -	---SD ☠	
<i>Tetraodon nigroviridis</i>	<u>C</u> ----	---N	--- <u>T</u> A	GG--Q ☠	
Homo sapiens	-----	---T	---M-	---G	

b)

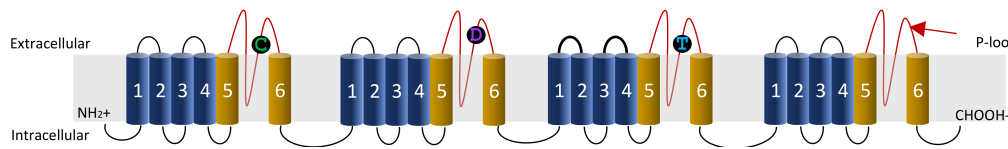
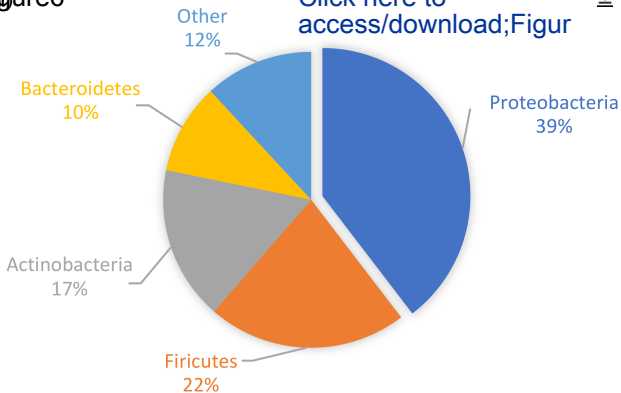
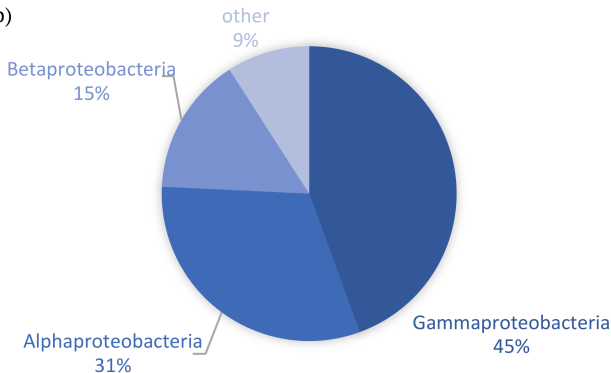


Figure 6

[Click here to access/download;Figur](#)



b)







[Click here to access/download](#)

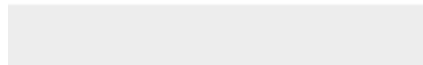
**Supplementary Material**

**SUPPLEMENTARY MATERIALS\_GS2\_5\_8\_2020.docx**





Click here to access/download  
**Supplementary Material**  
BRO Sequencing Insert Sizes.xlsx



Dear Dr. Goodman

I am pleased to submit an original research piece titled “**Adaptive venom evolution and toxicity in octopods is driven by extensive novel gene formation, expansion and loss**” for consideration to be published in *GigaScience*.

Much of cephalopod evolution remains unknown due to sparseness of their genomic sampling. Cephalopod genomes are some of the largest and most repetitive animal genomes and exhibit drastically different evolutionary trajectories relative to other better documented lineages. A more focused genomic study to reveal how individual genomic changes are associated with the evolution of novel organs, tissues, or adaptations, within a single group of cephalopods has been missing so far. We present such a study, focussing on adaptations in the toxic blue-ringed octopus the *Hapalochlaena maculosa*, for which we provide a high quality genome assembly based on multiple technologies. Members of the genus *Hapalochlaena* are the only octopods to contain the lethal neurotoxin, tetrodotoxin (TTX), within their venom and tissues and are a prime example of the origin of evolutionary novelties within octopods.

Using global comparative genomics approaches and focused study on TTX evolution, we report key findings:

- Gene family expansions crucial for the development of complex neural networks are present in cephalopods, yet are differentially expanding in all three octopod species
- Novel gene formation at different phylogenetic levels can be associated with evolution in a specific set of cephalopod tissues
- Changes in Posterior Salivary Gland composition (PSG) between TTX bearing and non-TTX bearing species
- Convergently evolved mutations consistent with TTX resistance detected in *H. maculosa*

We firmly believe that our manuscript is suited for publication by *GigaScience* as one of the first to explore the evolutionary genomic basis for novelties within octopods and cephalopods in general. Our whole genomic comparisons provide insight into the defining structure/features of octopod genomes at the species-specific level. Additionally, we

examine the impact of TTX on the evolution of venom in *H. maculosa* relative to non-TTX bearing octopods.

Yours sincerely,

Brooke L. Whitelaw  
James Cook University,  
Townsville, QLD 4810  
Mobile: 0424642621  
brooke.whitelaw@my.jcu.edu.au

Assoc. Prof. Jan Strugnell  
James Cook University,  
Townsville, QLD 4810  
jan.strugnell.jcu.edu.au

and

Prof. Oleg Simakov  
University of Vienna  
Universitätsring 1, 1010 Wien, Austria  
oleg.simakov@univie.ac.at